HHS Public Access

Author manuscript

Clin Cancer Res. Author manuscript; available in PMC 2020 August 25.

Published in final edited form as:

Clin Cancer Res. 2018 July 15; 24(14): 3423–3432. doi:10.1158/1078-0432.CCR-17-3406.

Targeting NAD+/PARP DNA Repair Pathway as a Novel Therapeutic Approach to *SDHB*-Mutated Cluster I Pheochromocytoma and Paraganglioma

Ying Pang[#1], **Yanxin Lu**[#2,3], **Veronika Caisova**[1,4], **Yang Liu**[2], **Petra Bullova**[1,5], **Thanh-Truc Huynh**[1], **Yiqiang Zhou**[2], **Di Yu**[2,6], **Zdenek Frysak**[7], **Igor Hartmann**[8], **David Taïeb**[9], **Karel Pacak**[#1], **Chunzhang Yang**[#2]

[1]Section on Medical Neuroendocrinology, Eunice Kennedy Shriver National Institute of Child Health and Human Development, National Institutes of Health, Bethesda, Maryland. [2]Neuro-Oncology Branch, Center for Cancer Research, National Cancer Institute, Bethesda, Maryland. [3]Basic Medical Science Department, Zunyi Medical College-Zhuhai Campus, Zhuhai, Guangdong, P.R. China. [4]Department of Medical Biology, Faculty of Science, University of South Bohemia, Ceske 19 Budejovice, Czech Republic. [5]Department of Molecular Medicine, Institute of Virology, Biomedical Research Center, Slovak Academy of Sciences, Bratislava, Slovakia. [6]CAS Key Laboratory of Separation Science for Analytical Chemistry, Dalian Institute of Chemical Physics, Chinese Academy of Sciences, Dalian, P.R. China. [7]3rd Department of Internal Medicine, University Hospital and Faculty of Medicine and Dentistry, Palacky University, Olomouc, Czech Republic. [8]Department of Urology, University Hospital Olomouc and Faculty of Medicine and Dentistry, Palacky University, Olomouc, Czech Republic. [9]Department of Nuclear Medicine, La Timone University Hospital, Centre Européen de Rechercheen Imagerie Médicale, Aix-Marseille University, Marseille, France.

[#] These authors contributed equally to this work.

Abstract

Corresponding Authors: Chunzhang Yang, National Cancer Institute, 37 Convent Drive, Room 1142, Bethesda, MD 20814. Phone: 240-760-7083; Fax: 240-541-4466; Chungzhang.Yang@nih.gov; and Karel Pacak, Eunice Kennedy Shriver NICHD, NIH, Building 10, CRC, 1E-3140, 10 Center Drive, MSC-1109, Bethesda, Maryland 20892-1109. Phone: 301-402-4594; Fax: 301-402-4712; karel@mail.nih.gov.

Authors' Contributions

Conception and design: Y. Pang, Y. Lu, K. Pacak, C. Yang

Development of methodology: Y. Pang, Y. Lu, Y. Liu, P. Bullova, C. Yang

Acquisition of data (provided animals, acquired and managed patients, provided facilities, etc.): Y. Pang, Y. Lu, V. Caisova, Y. Liu, T.-T. Huynh, I. Hartmann, K. Pacak, C. Yang

Analysis and interpretation of data (e.g., statistical analysis, biostatistics, computational analysis): Y. Pang, Y. Lu, Y. Zhou, D. Yu, D. Taieb, K. Pacak, C. Yang

Writing, review, and/or revision of the manuscript: Y. Pang, Y. Lu, Y. Liu, P. Bullova, I. Hartmann, D. Taieb, K. Pacak, C. Yang

Administrative, technical, or material support (i.e., reporting or organizing data, constructing databases): Y. Pang, Y. Lu, Y. Liu, Z. Frysak, I. Hartmann, K. Pacak, C. Yang

Study supervision: K. Pacak, C. Yang

Disclosure of Potential Conflicts of Interest

No potential conflicts of interest were disclosed.

Note: Supplementary data for this article are available at Clinical Cancer Research Online (http://clincancerres.aacrjournals.org/).

Purpose: Cluster I pheochromocytomas and paragangliomas (PCPGs) tend to develop malignant transformation, tumor recurrence, and multiplicity. Transcriptomic profiling suggests that cluster I PCPGs and other related tumors exhibit distinctive changes in the tricarboxylic acid (TCA) cycle, the hypoxia signaling pathway, mitochondrial electron transport chain, and methylation status, suggesting that therapeutic regimen might be optimized by targeting these signature molecular pathways.

Experimental Design: In the present study, we investigated the molecular signatures in clinical specimens from cluster I PCPGs in comparison with cluster II PCPGs that are related to kinase signaling and often present as benign tumors.

Results: We found that cluster I PCPGs develop a dependency to mitochondrial complex I, evidenced by the upregulation of complex I components and enhanced NADH dehydrogenation. Alteration in mitochondrial function resulted in strengthened NAD^+ metabolism, here considered as a key mechanism of chemoresistance, particularly, of succinate dehydrogenase subunit B (*SDHB*)-mutated cluster I PCPGs via the PARP1/BER DNA repair pathway. Combining a PARP inhibitor with temozolomide, a conventional chemotherapeutic agent, not only improved cytotoxicity but also reduced metastatic lesions, with prolonged overall survival of mice with *SDHB* knockdown PCPG allograft.

Conclusions: In summary, our findings provide novel insights into an effective strategy for targeting cluster I PCPGs, especially those with *SDHB* mutations.

Introduction

Pheochromocytomas and paragangliomas (PCPGs) are rare but life-threatening neoplasms that arise from the chromaffin tissue of the adrenal medulla and sympathetic ganglia (1). Transcriptomic profiling has identified two major clusters in PCPGs, designated as cluster I (signature associated with the activated hypoxia-angiogenesis signaling pathway) and cluster II (signature associated with activated MAPK and PI3K/AKT/mTOR signaling pathways) tumors (2, 3). In cluster I PCPGs, genetic abnormalities in metabolic pathways are frequently identified, such as succinate dehydrogenase (*SDHx*), von Hippel–Lindau tumor suppressor (*VHL*), hypoxia-inducible factor 2A (*HIF2A*), and fumarate hydratase (*FH*; ref. 4). In contrast, cluster II diseases are mainly associated with aberrations in kinase pathways, such as neurofibromatosis type I (*NF1*), ret proto-oncogene (*RET*), kinesin family member 1B (*KIF1B*), MYC-associated factor X (*MAX*), and transmembrane protein 127 (*TMEM127*; ref. 5). Cluster I PCPGs exhibit substantial changes in molecular pathways of the TCA cycle, electron transport chain, and hypoxia signaling, suggesting distinctive mitochondrial reprogramming in cluster I PCPGs and other tumors (6). Taking *SDHx*-mutated PCPG as an example, the disruption of complex II triggers abnormal ROS generation in the mitochondrial matrix, which leads to tumorigenesis via the activation of the hypoxia-inducible factor α (HIFα; ref. 7). Despite being usually benign, overall about 10% to 15% PCPGs develop distant metastasis and are considered malignant (4, 8). Among genetic alterations in PCPGs, mutations in succinate dehydrogenase (*SDHx*) predispose patients to aggressive phenotypes, such as distal metastasis, in some series in up to 70% of patients, and tumor multiplicity and recurrence, which emphasizes an urgent need for effective therapies against *SDHx*-mutated PCPGs (9).

The current standard of care for metastatic PCPGs includes chemotherapy, radiation therapy, and surgical resection (10, 11). Chemotherapy with a combination regimen of cyclophosphamide–vincristine–dacarbazine (CVD) is recommended to manage advanced PCPGs (12). CVD therapy results in tumor regression and symptom relief in around 50% of cases, whereas the responses are usually transient (13), with only marginal survival benefit for PCPGs (12, 14). Temozolomide (TMZ), which has a similar safety profile and effects with the CVD component, dacarbazine, has been performed as an alternative genotoxic agent for multiple tumor types (15, 16). Furthermore, a recent pioneering study by Hadoux and colleagues suggested that TMZ might be more effective against metastatic PCPGs with *SDHB* mutations, implying that PCPGs might be better targeted based on their distinctive genetic background (17). However, there is a lack of understanding on how a therapeutic regimen could be optimized based on the guidance from the distinctive transcriptomic profile.

Many chemotherapeutic agents, including TMZ, trigger tumor cell apoptosis through damaging genomic DNA. Poly(ADP-ribose) polymerase (PARP) is a highly conserved enzyme in eukaryotes, which produces ADP-ribose–conjugated PARP (PADPR) to repair DNA breaks, stabilize DNA replication, and maintain chromatin integrity (18). PARP-deficient mice and cells showed DNA instability and were extremely sensitive to DNA-damaging agents (19). Thus, PARP inhibitors, which were demonstrated to potentiate DNA-damaging effect of chemotherapy agents (20, 21), could be promising pharmacological target for metastatic tumors.

In the present study, we investigated molecular signatures in clinical specimens from cluster I and II PCPGs. We also tested the applicability of a combination therapy using the PARP inhibitor olaparib (Ola) and TMZ in an allograft model. We found that *SDHB*-mutated PCPG exhibited reprogrammed mitochondrial complex I. Augmented complex I activity increased intracellular NAD^+ levels through enhanced catalytic activity of NADH dehydrogenase. Elevated NAD^+ serves as an important cofactor to support the PARP DNA repair pathway, resulted in chemoresistance in *SDHB*-associated PCPGs. Targeting the NAD^+/PARP DNA repair pathway with Ola not only sensitized cluster I PCPGs cells to genotoxic agents but also suppressed metastatic xenograft lesions and improves overall survival. Our results suggest that the NAD^+/PARP pathway is a crucial targetable pathway in *SDHB*-mutated PCPG. Combination therapy using TMZ and Ola could become an effective strategy against these and other cluster I metastatic tumors.

Materials and Methods

This study was approved by the Institutional Review Board of the *Eunice Kennedy Shriver* NICHD/NIH, and the index patient gave written informed consent.

Tumor specimen

Tumor samples were collected from clinical specimens of cluster I and cluster II PCPG patients.

Cell lines

Mouse metastatic PC tumor (MTT) cell line was established by our group as previously described (22). Cells were maintained in Dulbecco's Modified Eagle Medium (DMEM) supplemented with 10% fetal bovine serum (FBS), penicillin, and streptomycin. To generate an *SDHB*-deficient line (MTT-$SDHB^{KD}$ cells), MTT cells were transduced by lentivirus with short hairpin RNA targeting *SDHB* (SH-042339–2-10, targeting sequence TGA GTA ACT TCT ACG CAC A, GE Dharmacon). Isogenic cells were selected by puromycin, and knockdown efficiency was evaluated by Western blot. MTT cells with *SDHB* knockdown were further transfected with pcDNA 3.1-cytomegalovirus-firefly luciferase plasmid enriched by G418 selection (MTT-$SDHB^{KD}$-Luc cells).

Immunohistochemistry

Formalin-fixed, paraffin-embedded tissue specimen was prepared for 5-μm sections. Tissue section was deparaffinized and rehydrated in xylene and ethanol, respectively. Sections were subjected to heat-induced antigen retrieval at 95°C for 20 minutes. Specimens were incubated with primary antibody overnight at 4°C. HRP-conjugated anti-rabbit IgG or anti-mouse IgG secondary antibody were incubated with the specimens and developed by DAB substrate. Slides were counter-stained by hematoxylin and dehydrated by a series of graded ethanol. The primary antibodies used for immunohistochemistry include NDUFS2 (Novus, NBP2–30413, 1:200), NDUFS3 (Novus, H00004722-M02, 1:150), NDUFB6 (Novus, NBP1–92172, 1:200), PARP (Abcam, ab32138, 1:50), and pADPR (Abcam, ab14459, 1:100).

Western blotting

Protein was extracted from cell culture or tissues specimen using RIPA lysis buffer supplemented with protease inhibitor cocktail (Thermo Fisher Scientific). The BCA Protein Assay Kit (Thermo Fisher Scientific) was used to determine protein content. Equal amounts of proteins were separated in NuPAGE 4% to 12% minigels (Life Technologies) and transferred to PVDF membranes (Bio-Rad). Membrane was incubated with primary antibody overnight at 4°C and visualized by HRP/chemiluminescence kit (Thermo Fisher Scientific). The primary antibodies used in the present study include NDUFS2 (Novus, NBP2–30413, 1:500 dilution), NDUFS3 (Abcam, ab110246, 1:1,000), NDUFSB6 (Novus, NBP1–92172, 1:500), PARP (CST, 9542S, 1:1,000), pADPR (Abcam, ab14459, 1:500), and β-Actin (CST, 4970S, 1:5,000).

RNA extraction and quantitative PCR analysis

Total RNA was extracted from cells using RNeasy Mini Kit (Qiagen). One microgram RNA was reversely transcribed to cDNA by SuperScript III first-strand synthesis SuperMix (Life technologies). Real-time PCR was carried out using the power SYBR Green PCR Master Mix Kit (Life technologies) on ViiA7 Real-Time PCR system (Life Technologies). The RT^2 $Profiler^T$ PCR Array for mouse mitochondrial energy metabolism was purchased from Qiagen (Catalog# PAMM-008ZA-2).

Cell-cycle analysis

One million cells were seeded on 6-well plates for cell-cycle analysis. Cells were collected and fixed using 75% ethanol overnight at −20°C. Cellular DNA content was probed with propidium iodide. Stained cells were analyzed by FACS canto II (BD Biosciences) flow cytometer.

Apoptosis analysis

Cell apoptosis was analyzed by evaluating the levels of cleaved PARP1 and active caspases by Apoptosis Antibody Sampler Kit (Cell Signaling Technology) and caspase-Glo 3/7 Assay Systems (Promega) according to the manufacturer's protocol.

DNA fragmentation assay

Genomic DNA was extracted from the control and treated cells using DNeasy Blood & Tissue Kit (QIAGEN) according to the manufacture's protocol. Five hundred nanogram DNA samples were mixed with loading dye and were resolved by electrophoresis on a 4% to 20% Novex TBE gel (Thermo Fisher Scientific). The gel was stained with SYBR safe DNA Gel Dye (Life Technologies) and visualized using Bio-Rad ChemiDoc Imaging system.

Alkaline Comet assay

Alkaline Comet assay was performed to detect the DNA damage due to apoptosis, as previously described (23). Cells were mixed with low-temperature melting agarose and spread on the slides. The slides were submerged in lysis buffer then subjected to electrophoresis at a voltage of 1 V/cm for 20 minutes. After electrophoresis, slides were stained by SYBR Safe DNA Gel for 20 minutes and visualized by the fluorescence microscopy.

In vivo allograft animal model

The animal experiments were approved by the *Eunice Kennedy Shriver* NICHD animal protocol (ASP: 15–028). Six-week-old female nude athymic mice were injected 1.5 million MTT-$SDHB^{KD}$-Luc cells suspended in 100-μL PBS through the tail vein. Seven days after inoculation, tumor growth was evaluated by IVIS imaging. Mice were then randomly divided into four groups and received intraperitoneal (i.p.) injections of PBS, TMZ, Olaparib, or TMZ+Olaparib, respectively, from 10 days after tumor transplantation. TMZ was dissolved in DMSO, diluted in PBS (10 mg/mL), and injected intraperitoneally (50 mg/kg) every other day for four doses. Olaparib as administered intraperitoneally (10 mg/kg) for 8 days from the start of TMZ. After a 2-week interval, compounds were performed for the next round. Mice were monitored every day and imaged by the IVIS system every week to measure tumor growth. At the end of experiments, all animals were sacrificed, and livers with tumors were resected and processed for histologic analysis.

Statistical analysis

All the statistical analyses were performed by GraphPad Prism software (v7.0) and Excel (Microsoft). One-way ANOVA followed by Student *t* test as the poststatistical analysis. In

all instances, data were shown as mean ± SEM. *, $P < 0.05$ was considered as statistically significant.

Results

Upregulation of complex I activity in cluster I PCPGs

To better understand the alteration in mitochondrial complexes in PCPGs, we investigated the expression level of complex I components among normal adrenal medulla and cluster I and II PCPGs. The expression of mitochondrial complex I core subunits NDUFS2, NDUFS3, and the core accessory subunit NDUFB6 were found to be upregulated in cluster I samples (Fig. 1A). Higher expression levels of complex I components were confirmed by quantitative analysis and Western blotting (Fig. 1B and C). To better understand whether the upregulation of mitochondrial complex I components correlates with cluster I PCPG pathogenic mutations, we established an *SDHB* knockdown cell line by stably expressing shRNA in a mouse metastatic PC cell line, MTT. Quantitative PCR confirmed that the expression levels of *SDHB* were extensively downregulated in the $SDHB^{KD}$ cell line, with a corresponding elevation in hypoxia-related genes and mitochondrial complex I components, indicating augmented complex I function with SDHx deficiency (Fig. 1D; Supplementary Fig. S1A). Western blot analysis of the $SDHB^{KD}$ cell line confirmed that the complex I components NDUFS2, NDUFS3, and NDUB6 were upregulated in the $SDHB^{KD}$ cell line (Fig. 1E). A direct measurement of complex I activity revealed an elevation in mitochondrial complex I activity in $SDHB^{KD}$ cells. Activities of complex I were suppressed to the baseline level by metformin, as the inhibitor of complex I in both $SDHB^{WT}$ and $SDHB^{KD}$cells (Fig. 1F).

Mitochondrial complex I dependency potentiates NAD metabolism via NADH dehydrogenation

Mitochondrial complex I catalyzes the first step of the electron transport chain and oxidizes NADH to NAD^+ (24). Increased expression of mitochondrial complex I components suggests NADH dehydrogenation and altered NAD^+ levels in cluster I PCPGs. To test this hypothesis, we first measured NAD^+/NADH levels in patient-derived tumor samples. The quantity of NAD^+ in cluster I tumors was found to be 2.7-fold higher than that in cluster II tumors (Fig. 2A). Furthermore, we confirmed this finding *in vitro* using the $SDHB^{KD}$ cell line; increased NAD^+ levels were identified in both whole cells and the mitochondrial compartment of $SDHB^{KD}$ cells (Fig. 2B and C). In addition, we demonstrated that enhanced mitochondrial complex I activity is responsible for a strengthened pool of NAD^+ metabolism in $SDHB^{KD}$ cells, as NAD^+ level could be suppressed by metformin, or Nampt governed NAD^+ salvage pathway inhibitors, in $SDHB^{KD}$ cells (Fig. 2D; Supplementary Fig. S1B). Native blue gel analysis and in-gel enzyme activity assay confirmed that $SDHB^{KD}$ cells exhibited augmented complex I formation and activity (Supplementary Fig. S1C).

Strengthened NAD^+ metabolism establishes chemoresistance through PARP DNA repair

NAD^+ is an important substrate for PARP to transfer the ADP-ribose residues to synthesize pADPR, which helps DNA repair and rescues tumor cells from DNA damaged-associated cell death (25, 26). To study whether higher NAD^+ levels affect PARP DNA repair in cluster

I PCPGs, we first compared PARP/pADPR levels in patient tumor specimens. We identified a significant elevation in pADPR level in cluster I PCPGs, which implied that PARP DNA repair is affected by the increased availability of NAD^+ (Fig. 2E). Furthermore, we identified enhanced pADPR formation in *SDHB*^{KD} cells (Fig. 2F). The level of pADPR could be modulated by exogenous NAD^+ or NAD^+ depletion via the salvage pathway.

The alteration in the PARP DNA repair pathway suggested that cluster I PCPG may exploit enhanced NAD^+ metabolism as a mechanism of chemoresistance. To test this, we assessed pADPR formation in the presence of the genotoxic agent TMZ. We found that TMZ treatment induced a conspicuous elevation in pADPR levels *in vitro*. Stronger pADPR induction was seen in *SDHB*^{KD} cells, indicating that TMZ-induced DNA damage is handled more efficiently in these cells (Fig. 2G). We confirmed that *SDHB* deficiency correlated with more effective chemoresistance, as demonstrated by reduced γH2A.X staining in the presence of TMZ (Fig. 2H and I). As a further validation, dose-dependent curves of cell viability revealed that *SDHB*^{KD} cells were more resistant to TMZ treatment. The IC_{50} of *SDHB*^{KD} cells was 731 μmol/L, whereas the IC_{50} of *SDHB*^{WT} cells was found to be 357 μmol/L (Fig. 2J). In addition, we found the potentiated drug resistance is closely linked to SDHB deficiency, as reexpression of SDHB expressing vector partially reduced the quantity of NAD+ and pADPR, with a corresponding with elevated DNA damage shown as γH2A.X expression (Fig. S1D and S1E).

Targeting the PARP DNA repair pathway potentiates the therapeutic effect of genotoxic agents

The correlation between SDHB deficiency and chemoresistance indicates that genotoxic agents might be more effective when PARP DNA repair is compromised. Thus, we evaluated the therapeutic effect of TMZ for *SDHB* PCPGs in the presence of the FDA-approved PARP inhibitor Ola (27). MTT cells were treated with a combination of TMZ and Ola. We found that TMZ robustly induced pADPR formation in SDHB-deficient cells, suggesting that enhanced NAD^+ metabolism supports DNA damage detoxification (Fig. 3A). Ola completely abolished the formation of pADPR in both *SDHB*^{WT} and *SDHB*^{KD} cells. We recorded corresponding enhanced DNA damage when Ola was included in the treatment, evidenced by a stronger γH2A.X signal by Western blotting and immunostaining assays (Fig. 3A and B). Quantitative analysis of the γH2A.X signal demonstrated that Ola increased TMZ-induced DNA damage by 46.8% (*SDHB*^{WT}) and 244.9% (*SDHB*^{KD}) in MTT cells (Fig. 3C). As a further validation, we observed increased DNA fragmentation by DNA electrophoresis and comet assay (Fig. 3D and E). Combined Ola and TMZ treatment resulted in more fragmented DNA in both *SDHB*^{WT} and *SDHB*^{KD} cells. By measuring the tail moment in the comet assay, we confirmed that inhibition of the PARP DNA repair pathway resulted in 62.6% (*SDHB*^{WT}) and 225.7% (*SDHB*^{KD}) increase in DNA fragmentation in MTT cells (Fig. 3F). To better understand whether the combination therapy would achieve stronger cytotoxicity in MTT cells, we investigated PARP and caspase cleavage under Ola and TMZ treatment (Fig. 3G). Western blot analysis showed that MTT cells with SDHB deficiency are less likely to proceed to apoptosis under TMZ treatment alone. Ola plus TMZ combination therapy led to marked cleavage of PARP and caspase-3, suggesting that more cells underwent apoptotic changes due to the accumulation of DNA

damage. In line with this finding, the caspase-3/7 cleavage assay showed that Ola increased TMZ-induced apoptotic changes by 135.4% in *SDHB*^{WT} and 116.4% in *SDHB*^{KD} (Fig. 3H). The therapeutic effect of the combination therapy was further verified by cell-cycle analysis (Fig. 3I; Supplementary Fig. S1F). A significant G_2–M arrest was recorded when cells were treated with Ola and TMZ (75.2% for *SDHB*^{WT} cells, 62.1% for *SDHB*^{KD} cells). In the present study, we did not detect MGMT expression in MTT cell lines, suggesting MGMT pathway is not involved in the chemoresistance in our cellular models (Supplementary Fig. S1G).

Combination of a PARP inhibitor and TMZ relieves tumor burden and metastatic lesions of SDHB-mutated PCPGs

Our findings suggest that mitochondrial reprogramming results in chemoresistance in cluster I PCPGs via an NAD^+/PARP-dependent pathway. We proposed that using PARP inhibitors could be an effective therapy for *SDHx*/cluster I PCPGs by targeting the major chemoresistance mechanism. Thus, we first evaluated *SDHB*^{KD} MTT cell viability under combination therapy (Fig. 4A; Supplementary Fig. S1H). Combining Ola reduced the IC_{50} of TMZ from 731 μmol/L to 311 μmol/L. Moreover, the combination therapy resulted in less BrdU incorporation in *SDHB*^{WT} and *SDHB*^{KD} cells *in vitro*, suggesting an effective suppression in tumor progression (Fig. 4B).

We further evaluated the sensitizing effect of Ola in a metastatic PC in an allograft model. Ola treatment alone did not show notable suppressive effects on tumor growth (Fig. 4C). Bioluminescence imaging showed that the tumor growth rate was slightly reduced with TMZ treatment (Fig. 4D). However, remarkable tumor suppression was detected in the TMZ and Ola combination group. Five weeks after tumor allograft, about 70% and 49% tumor growth was suppressed in the combination group, compared with the DMSO and TMZ groups, respectively (Supplementary Fig. S1I). In addition, combining Ola with TMZ exhibited a survival benefit, as shown by a significant increase in mouse survival in the combination group (median survival: 52 days) compared with TMZ injection alone (median survival: 42 days, $P = 0.0028$; Fig. 4E). Histologic sections from four groups showed a robust increase in γH2A.X and cleaved caspase-3 in the tumor sections from the combination group (Fig. 4F). No obvious drug toxicity was observed from the experimental animals.

Discussion

Cluster I PCPGs exhibit aggressive phenotypes such as tumor progression, multiplicity, recurrence, and metastasis. Therefore, effective therapies are warranted to handle cluster I PCPGs more efficiently to improve patient outcome and overall survival. Here, we describe new insights into the distinctive metabolic pathways in cluster I PCPGs. Cluster I PCPGs develop dependency toward mitochondrial complex I, which results in resistance to chemotherapy by augmented NAD^+ metabolism and PARP DNA repair pathway activation (Fig. 5). The combination of an FDA-approved PARP inhibitor, Ola, with TMZ chemotherapy show promising therapeutic effects against cluster I PCPGs, demonstrated by profound cytotoxicity in PCPG cells, as well as suppressed metastatic allograft lesions and

longer overall survival of mice with PCPG allograft. Our findings highlight a novel therapeutic regimen that could benefit patients with cluster I metastatic PCPGs.

Mitochondrial reprogramming contributes to chemoresistance

Mitochondrial function is essential for energy metabolism and macromolecule synthesis (28, 29). The unexpected finding that *SDHB* depletion resulted in reprogrammed expression of the mitochondrial complex suggested fundamental changes in mitochondrial function that are unique to cluster I PCPGs (Fig. 1). Mitochondrial complexes I and II are critical for the electron transport chain, which donates free electrons to ubiquinone via the Fe-S cluster. Previous findings suggested that dysfunction in mitochondrial complex II leads to abnormal mitochondrial morphology, ROS generation, and DNA hypermethylation phenotypes (9, 30, 31). However, the direct impact of *SDHx* mutations to physiologic mitochondrial function is not fully understood. In the present study, we showed that in cluster I PCPGs, the deficiency of mitochondrial complex II may reduce electron availability for proper mitochondrial function (Fig. 1). The hyperactivation of complex I might function as a compensatory mechanism to maintain electron input and mitochondrial membrane potential. Enhanced mitochondrial complex I activity resulted in elevated NADH dehydrogenation, which altered the NAD^+/NADH balance (Fig. 2A–D). Furthermore, we demonstrated that increased NAD^+ availability was linked to the resistance mechanism for *SDHB*-mutated PCPG, as NAD^+ levels closely correlated with the expression level of pADPR and the accumulation of DNA damage (Fig. 2E–J). Overall, these findings suggest a novel resistance mechanism in *SDHB*-mutated PCPG.

PARP inhibitors restore sensitivity to genotoxic agents

Base excision repair (BER) plays a vital role in repairing genotoxic agent-induced DNA lesions by processing short-patch or long-patch BER (32). PARP governs the BER pathway and maintains genomic integrity during chemotherapy (33). Inhibition of PARP has been proposed for patients with dysfunctional homologous recombination to maintain or improve the chemotherapy response (34). In addition, PARP inhibition sensitizes hepatocellular carcinoma cells to arsenic trioxide treatment (35). Recent studies found that NAD^+ depletion could be a novel strategy to suppress the PARP/BER pathway and improve the effect of conventional chemotherapy (36, 37). In the present study, we identified a novel chemoresistance mechanism in *SDHB*-mutated PCPGs through the enhancement of the BER/PARP DNA repair pathway, demonstrated by the increased expression of pADPR in cluster I PCPGs (Fig. 2E and G). Moreover, *SDHB* depletion was found to be closely linked to reduced DNA damage and apoptotic changes under genotoxic agents, suggesting a distinctive SDHB-resistant mechanism (Fig. 2H–J). A more careful investigation indicated that SDHB deficiency augmented the PARP/BER pathway via potentiated NADH dehydrogenase activity in the mitochondrial matrix, suggesting that NAD^+ metabolism could be a novel target for cluster I PCPGs (Fig. 2F). Our finding highlighted that combining PARP inhibition with the present chemotherapy regimen might restore effectiveness against cluster I PCPGs.

Combination of a PARP inhibitor and TMZ suppressed *SDHB*-mutated PCPGs

PCPGs are generally considered incurable when they advance to malignant stages, and the current therapeutic approaches for such tumors are limited (10). The standard care for PCPGs includes surgery or chemotherapy, following the CVD regimen. When surgery is not an option, especially in rapidly growing metastatic PCPGs, chemotherapy is the only applicable therapeutic approach (38). However, the CVD strategy only provides transient symptom relief and marginal improvement in overall survival in advanced PCPGs (14). In an earlier study, the mTOR inhibitor everolimus (RAD001) was tested in four patients with progressive metastatic cluster II PCPGs; however, the results were not promising (39). Furthermore, targeting mTORC1/2 pathways by a selective ATP-competitive inhibitor showed promising tumor suppression in mouse models (40). A retrospective study on cluster I PCPGs showed that these tumors might respond better to sunitinib, a multitargeted receptor tyrosine kinase inhibitor, suggesting that PCPGs show a varied spectrum of vulnerability depending on the genetic background (41). Cluster I mutations (*SDHx*), especially *SDHB* mutations, might be related to malignancy and poor prognosis (42), and about half of the patients with metastatic extra-adrenal PGs carry pathogenic *SDHB* mutations (43). Therefore, more efficient chemotherapies need to be developed for metastatic PCPGs, especially for targeting cluster I tumors.

TMZ is a DNA-alkylating compound, which is widely applied in treating malignant tumors, including glioblastomas, pituitary adenomas, and carcinomas (44, 45). Combining chemosensitizers has been shown to profoundly improve the therapeutic effect of TMZ in different tumor models. For example, suppressing protein phosphatase 2 (PP2A) sensitizes PC to TMZ treatment *in vitro* and *in vivo* (22). In a phase II study, TMZ in combination with the targeted drug thalidomide was used for malignant neuroendocrine tumors. The results showed that 33% PC patients responded to the regimen; however, the cytotoxic effect was reported in other endocrine malignancies (46). Chloroquine and vitamin P were also demonstrated to sensitize malignant gliomas/glioblastomas to TMZ treatment by blocking autophagy (47, 48). A recent study combined an ATM kinase inhibitor with TMZ to treat brain cancer and found that this combination sensitized highly resistant glioma cells to chemotherapies (49). The combination of a NAD^+/PARP inhibitor with TMZ is a recently developed chemotherapy regimen, which has shown promising effects against gliomas with pathogenic *IDH1* mutations (36, 37, 50, 51). Furthermore, PARP inhibitor was found sensitizing chemoresistant malignant melanoma for TMZ administration (52). In Ewing's Sarcoma, PARP inhibitor was reported to enhance the response to TMZ treatment and clinical trials with this combination for Ewing's Sarcoma treatment are currently in process (53). In the present study, we found that *SDHB* deficiency led to chemoresistance by enhancing the NAD^+/PARP DNA repair pathway (Fig. 2), suggesting that NAD^+/PARP inhibitors might constitute a tenable approach to support genotoxic agents, as more DNA damage can be accumulated when the major chemoresistant pathway is compromised. Our *in vitro* findings demonstrated that the combination therapy conferred promising effects by enhanced DNA damage, cellular apoptosis, and reduced IC_{50} under TMZ treatment (Fig. 3). In addition, through the metastatic allograft animal model, we showed that the combination of a PARP inhibitor and TMZ effectively reduced tumor proliferation, metastatic lesions, and aggressive phenotypes *in vivo* (Fig. 4). Our results highlighted a possible combination

regimen unique to cluster I PCPGs, which might be extended to clinical trials for patients with metastatic PCPGs, especially for chemoresistant patients carrying *SDHB* mutations.

Acknowledgments

This research was supported by the Intramural Research Program of the NIH, National Cancer Institute (NCI), Center for Cancer Research (CCR), and the *Eunice Kennedy Shriver* National Institute of Child Health and Human Development (NICHD). We would like to acknowledge Dr. Mark R. Gilbert of the Neuro Oncology Branch, CCR, NCI in the production of this article. We would like to acknowledge Vivian Diaz and Brenda Klaunberg, i*n vivo* NMR Center, NINDS, by providing technical assistance in animal imaging.

References

1. Pasini B, Stratakis CA. SDH mutations in tumorigenesis and inherited endocrine tumours: lesson from the phaeochromocytoma-paraganglioma syndromes. J Intern Med 2009;266:19–42. [PubMed: 19522823]
2. Eisenhofer G, Huynh TT, Pacak K, Brouwers FM, Walther MM, Linehan WM, et al. Distinct gene expression profiles in norepinephrine- and epinephrine-producing hereditary and sporadic pheochromocytomas: activation of hypoxia-driven angiogenic pathways in von Hippel-Lindau syndrome. Endocr Relat Cancer 2004;11:897–911. [PubMed: 15613462]
3. Favier J, Brière JJ, Burnichon N, Rivière J, Vescovo L, Benit P, et al. The Warburg effect is genetically determined in inherited pheochromocytomas. PLoS One 2009;4:e7094. [PubMed: 19763184]
4. Vicha A, Taieb D, Pacak K. Current views on cell metabolism in SDHx-related pheochromocytoma and paraganglioma. Endocr Relat Cancer 2014;21:R261–77. [PubMed: 24500761]
5. Favier J, Amar L, Gimenez-Roqueplo AP. Paraganglioma and phaeochromocytoma: from genetics to personalized medicine. Nat Rev Endocrinol 2015;11:101–11. [PubMed: 25385035]
6. Dahia PL, Ross KN, Wright ME, Hayashida CY, Santagata S, Barontini M, et al. A HIF1alpha regulatory loop links hypoxia and mitochondrial signals in pheochromocytomas. PLoS Genet 2005;1:72–80. [PubMed: 16103922]
7. Guzy RD, Sharma B, Bell E, Chandel NS, Schumacker PT. Loss of the SdhB, but Not the SdhA, subunit of complex II triggers reactive oxygen species-dependent hypoxia-inducible factor activation and tumorigenesis. Mol Cell Biol 2008;28:718–31. [PubMed: 17967865]
8. Ayala-Ramirez M, Feng L, Johnson MM, Ejaz S, Habra MA, Rich T, et al. Clinical risk factors for malignancy and overall survival in patients with pheochromocytomas and sympathetic paragangliomas: primary tumor size and primary tumor location as prognostic indicators. J Clin Endocrinol Metab 2011;96:717–25. [PubMed: 21190975]
9. Castro-Vega LJ, Letouzè E, Burnichon N, Buffet A, Disderot PH, Khalifa E, et al. Multi-omics analysis defines core genomic alterations in pheochromocytomas and paragangliomas. Nat Commun 2015;6:6044. [PubMed: 25625332]
10. Fliedner SM, Lehnert H, Pacak K. Metastatic paraganglioma. Semin Oncol 2010;37:627–37. [PubMed: 21167381]
11. Pang Y, Yang C, Schovanek J, Wang H, Bullova P, Caisova V, et al. Anthracyclines suppress pheochromocytoma cell characteristics, including metastasis, through inhibition of the hypoxia signaling pathway. Oncotarget 2017;8:22313–24. [PubMed: 28423608]
12. Huang H, Abraham J, Hung E, Averbuch S, Merino M, Steinberg SM, et al. Treatment of malignant pheochromocytoma/paraganglioma with cyclophosphamide, vincristine, and dacarbazine: recommendation from a 22-year follow-up of 18 patients. Cancer 2008;113:2020–8. [PubMed: 18780317]
13. Averbuch SD, Steakley CS, Young RC, Gelmann EP, Goldstein DS, Stull R, et al. Malignant pheochromocytoma: effective treatment with a combination of cyclophosphamide, vincristine, and dacarbazine. Ann Intern Med 1988;109:267–73. [PubMed: 3395037]

14. Nomura K, Kimura H, Shimizu S, Kodama H, Okamoto T, Obara T, et al. Survival of patients with metastatic malignant pheochromocytoma and efficacy of combined cyclophosphamide, vincristine, and dacarbazine chemotherapy. J Clin Endocrinol Metab 2009;94:2850–6. [PubMed: 19470630]
15. Villano JL, Seery TE, Bressler LR. Temozolomide in malignant gliomas: current use and future targets. Cancer Chemother Pharmacol 2009;64: 647–55. [PubMed: 19543728]
16. Agarwala SS, Kirkwood JM. Temozolomide, a novel alkylating agent with activity in the central nervous system, may improve the treatment of advanced metastatic melanoma. Oncologist 2000;5:144–51. [PubMed: 10794805]
17. Hadoux J, Favier J, Scoazec JY, Leboulleux S, Al Ghuzlan A, Caramella C, et al. SDHB mutations are associated with response to temozolomide in patients with metastatic pheochromocytoma or paraganglioma. Int J Cancer 2014;135:2711–20. [PubMed: 24752622]
18. Ray Chaudhuri A, Nussenzweig A. The multifaceted roles of PARP1 in DNA repair and chromatin remodelling. Nat Rev Mol Cell Biol 2017;18:610–21. [PubMed: 28676700]
19. de Murcia JM, Niedergang C, Trucco C, Ricoul M, Dutrillaux B, Mark M, et al. Requirement of poly(ADP-ribose) polymerase in recovery from DNA damage in mice and in cells. Proc Natl Acad Sci U S A 1997;94:7303–7. [PubMed: 9207086]
20. Ben-Hur E, Utsumi H, Elkind MM. Inhibitors of poly (ADP-ribose) synthesis enhance radiation response by differentially affecting repair of potentially lethal versus sublethal damage. Br J Cancer Suppl 1984; 6:39–42. [PubMed: 6230094]
21. Schlicker A, Peschke P, Bürkle A, Hahn EW, Kim JH. 4-Amino-1,8-naphthalimide: a novel inhibitor of poly(ADP-ribose) polymerase and radiation sensitizer. Int J Radiat Biol 1999;75:91–100. [PubMed: 9972795]
22. Martiniova L, Lu J, Chiang J, Bernardo M, Lonser R, Zhuang Z, et al. Pharmacologic modulation of serine/threonine phosphorylation highly sensitizes PHEO in a MPC cell and mouse model to conventional chemotherapy. PLoS One 2011;6:e14678.
23. Lu Y, Liu Y, Yang C. Evaluating in vitro DNA damage using comet assay. J Vis Exp 2017;128:e56450.
24. Hunte C, Zickermann V, Brandt U. Functional modules and structural basis of conformational coupling in mitochondrial complex I. Science 2010;329:448–51. [PubMed: 20595580]
25. Satoh MS, Lindahl T. Role of poly(ADP-ribose) formation in DNA repair. Nature 1992;356:356–8. [PubMed: 1549180]
26. Helleday T, Petermann E, Lundin C, Hodgson B, Sharma RA. DNA repair pathways as targets for cancer therapy. Nat Rev Cancer 2008;8:193–204. [PubMed: 18256616]
27. Ledermann J, Harter P, Gourley C, Friedlander M, Vergote I, Rustin G, et al. Olaparib maintenance therapy in platinum-sensitive relapsed ovarian cancer. N Engl J Med 2012;366:1382–92. [PubMed: 22452356]
28. Chan DC. Mitochondria: dynamic organelles in disease, aging, and development. Cell 2006;125:1241–52. [PubMed: 16814712]
29. Lin MT, Beal MF. Mitochondrial dysfunction and oxidative stress in neurodegenerative diseases. Nature 2006;443:787–95. [PubMed: 17051205]
30. Saito Y, Ishii KA, Aita Y, Ikeda T, Kawakami Y, Shimano H, et al. Loss of SDHB elevates catecholamine synthesis and secretion depending on ROS production and HIF stabilization. Neurochem Res 2016;41:696–706. [PubMed: 26620190]
31. Cervera AM, Apostolova N, Crespo FL, Mata M, McCreath KJ. Cells silenced for SDHB expression display characteristic features of the tumor phenotype. Cancer Res 2008;68:4058–67. [PubMed: 18519664]
32. Liu Y, Prasad R, Beard WA, Kedar PS, Hou EW, Shock DD, et al. Coordination of steps in single-nucleotide base excision repair mediated by apurinic/apyrimidinic endonuclease 1 and DNA polymerase beta. J Biol Chem 2007;282:13532–41. [PubMed: 17355977]
33. Ray Chaudhuri A, Nussenzweig A. The multifaceted roles of PARP1 in DNA repair and chromatin remodelling. Nat Rev Mol Cell Biol 2017;18:610–21. [PubMed: 28676700]
34. del Rivero J, Kohn EC. PARP inhibitors: the cornerstone of DNA repair-targeted therapies. Oncology (Williston Park) 2017;31:265–73. [PubMed: 28412778]

35. Luo Q, Li Y, Deng J, Zhang Z. PARP-1 inhibitor sensitizes arsenic trioxide in hepatocellular carcinoma cells via abrogation of G2/M checkpoint and suppression of DNA damage repair. Chem Biol Interact 2015;226:12–22. [PubMed: 25499136]
36. Tateishi K, Wakimoto H, Iafrate AJ, Tanaka S, Loebel F, Lelic N, et al. Extreme vulnerability of IDH1 mutant cancers to NAD+ depletion. Cancer Cell 2015;28:773–84. [PubMed: 26678339]
37. Tateishi K, Wakimoto H, Cahill DP. IDH1 mutation and world health organization 2016 diagnostic criteria for adult diffuse gliomas: advances in surgical strategy. Neurosurgery 2017;64:134–8. [PubMed: 28899049]
38. Keiser HR, Goldstein DS, Wade JL, Douglas FL, Averbuch SD. Treatment of malignant pheochromocytoma with combination chemotherapy. Hypertension 1985;7:I18–24. [PubMed: 3997232]
39. Druce MR, Kaltsas GA, Fraenkel M, Gross DJ, Grossman AB. Novel and evolving therapies in the treatment of malignant phaeochromocytoma: experience with the mTOR inhibitor everolimus (RAD001). Horm Metab Res 2009;41:697–702. [PubMed: 19424940]
40. Giubellino A, Bullova P, Nölting S, Turkova H, Powers JF, Liu Q, et al. Combined inhibition of mTORC1 and mTORC2 signaling pathways is a promising therapeutic option in inhibiting pheochromocytoma tumor growth: in vitro and in vivo studies in female athymic nude mice. Endocrinology 2013;154:646–55. [PubMed: 23307788]
41. Ayala-Ramirez M, Chougnet CN, Habra MA, Palmer JL, Leboulleux S, Cabanillas ME, et al. Treatment with sunitinib for patients with progressive metastatic pheochromocytomas and sympathetic paragangliomas. J Clin Endocrinol Metab 2012;97:4040–50. [PubMed: 22965939]
42. King KS, Prodanov T, Kantorovich V, Fojo T, Hewitt JK, Zacharin M, et al. Metastatic pheochromocytoma/paraganglioma related to primary tumor development in childhood or adolescence: significant link to SDHB mutations. J Clin Oncol 2011;29:4137–42. [PubMed: 21969497]
43. Klein RD, Jin L, Rumilla K, Young WF Jr, Lloyd RV. Germline SDHB mutations are common in patients with apparently sporadic sympathetic paragangliomas. Diagn Mol Pathol 2008;17:94–100. [PubMed: 18382370]
44. Lee CY. Strategies of temozolomide in future glioblastoma treatment. Onco Targets Ther 2017;10:265–70. [PubMed: 28123308]
45. Almalki MH, Aljoaib NN, Alotaibi MJ, Aldabas BS, Wahedi TS, Ahmad MH, et al. Temozolomide therapy for resistant prolactin-secreting pituitary adenomas and carcinomas: a systematic review. Hormones (Athens) 2017; 16:139–49. [PubMed: 28742502]
46. Kulke MH, Stuart K, Enzinger PC, Ryan DP, Clark JW, Muzikansky A, et al. Phase II study of temozolomide and thalidomide in patients with metastatic neuroendocrine tumors. J Clin Oncol 2006;24:401–6. [PubMed: 16421420]
47. Golden EB, Cho HY, Jahanian A, Hofman FM, Louie SG, Schönthal AH, et al. Chloroquine enhances temozolomide cytotoxicity in malignant gliomas by blocking autophagy. Neurosurg Focus 2014;37:E12.
48. Zhang P, Sun S, Li N, Ho ASW, Kiang KMY, Zhang X, et al. Rutin increases the cytotoxicity of temozolomide in glioblastoma via autophagy inhibition. J Neurooncol 2017;132:393–400. [PubMed: 28293765]
49. Golding SE, Rosenberg E, Adams BR, Wignarajah S, Beckta JM, O'Connor MJ, et al. Dynamic inhibition of ATM kinase provides a strategy for glioblastoma multiforme radiosensitization and growth control. Cell Cycle 2012;11:1167–73. [PubMed: 22370485]
50. Lu Y, Kwintkiewicz J, Liu Y, Tech K, Frady LN, Su YT, et al. Chemosensitivity of IDH1-mutated gliomas due to an impairment in PARP1-Mediated DNA Repair. Cancer Res 2017;77:1709–18. [PubMed: 28202508]
51. Sulkowski PL, Corso CD, Robinson ND, Scanlon SE, Purshouse KR, Bai H, et al. 2-Hydroxyglutarate produced by neomorphic IDH mutations suppresses homologous recombination and induces PARP inhibitor sensitivity. Sci Transl Med 2017;9.
52. Tentori L, Leonetti C, Scarsella M, Muzi A, Vergati M, Forini O, et al. Poly(ADP-ribose) glycohydrolase inhibitor as chemosensitiser of malignant melanoma for temozolomide. Eur J Cancer 2005;41: 2948–57. [PubMed: 16288862]

53. Engert F, Schneider C, Weiβ LM, Probst M, Fulda S. PARP inhibitors sensitize ewing sarcoma cells to temozolomide-induced apoptosis via the mitochondrial pathway. Mol Cancer Ther 2015; 14:2818–30. [PubMed: 26438158]

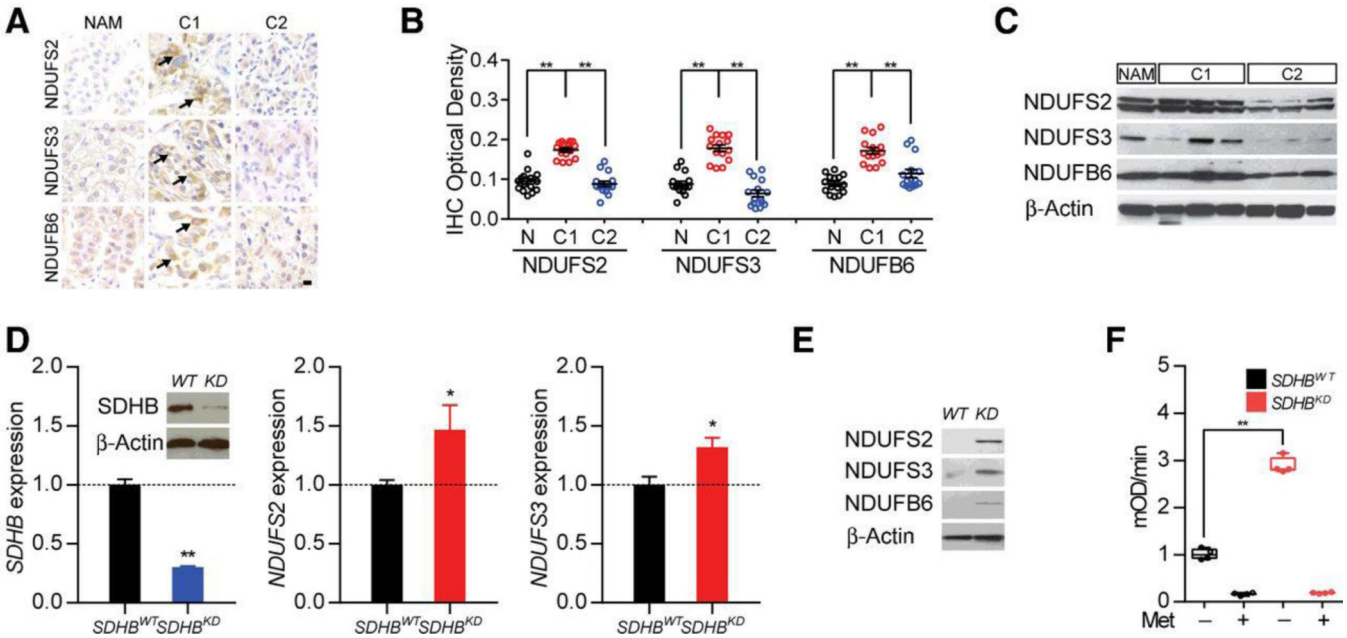

Figure 1.

Upregulation of mitochondrial complex I activity in cluster I PCPG. **A,** Immunohistochemistry of mitochondrial complex I components in cluster I (CI) and cluster II (CII) neuroendocrine tumor specimens showed upregulation of complex I subunits (NDUFS2, NDUFS3, and NDUFB6). Normal adrenal medulla (NAM) was used as control. Bar, 10 μm. **B,** Densiometric quantification of complex I components in CI and CII PCPG. **, $P < 0.01$. **C.** Western blot for the mitochondrial complex I components in CI and CII PCPGs confirmed overexpression of complex I. NAM was used as control. β-Actin was used as loading control. **D,** Quantitative PCR showed *SDHB, NDUFS2*, and *NDUFS3* expression in MTT cells. Higher expressions of complex I subunits were detected in $SDHB^{KD}$ cells. Western blotting showed over 60% knockdown efficiency of SDHB in MTT cells (inset). β-Actin was used as loading control. **E,** Western blotting for the mitochondrial complex I expression in MTT cells.β-Actin was used as loading control. **F,** Mitochondrial complex I assay showed much higher complex I activity level in $SDHB^{KD}$ cells than $SDHB^{WT}$ cells. **, $P < 0.01$.

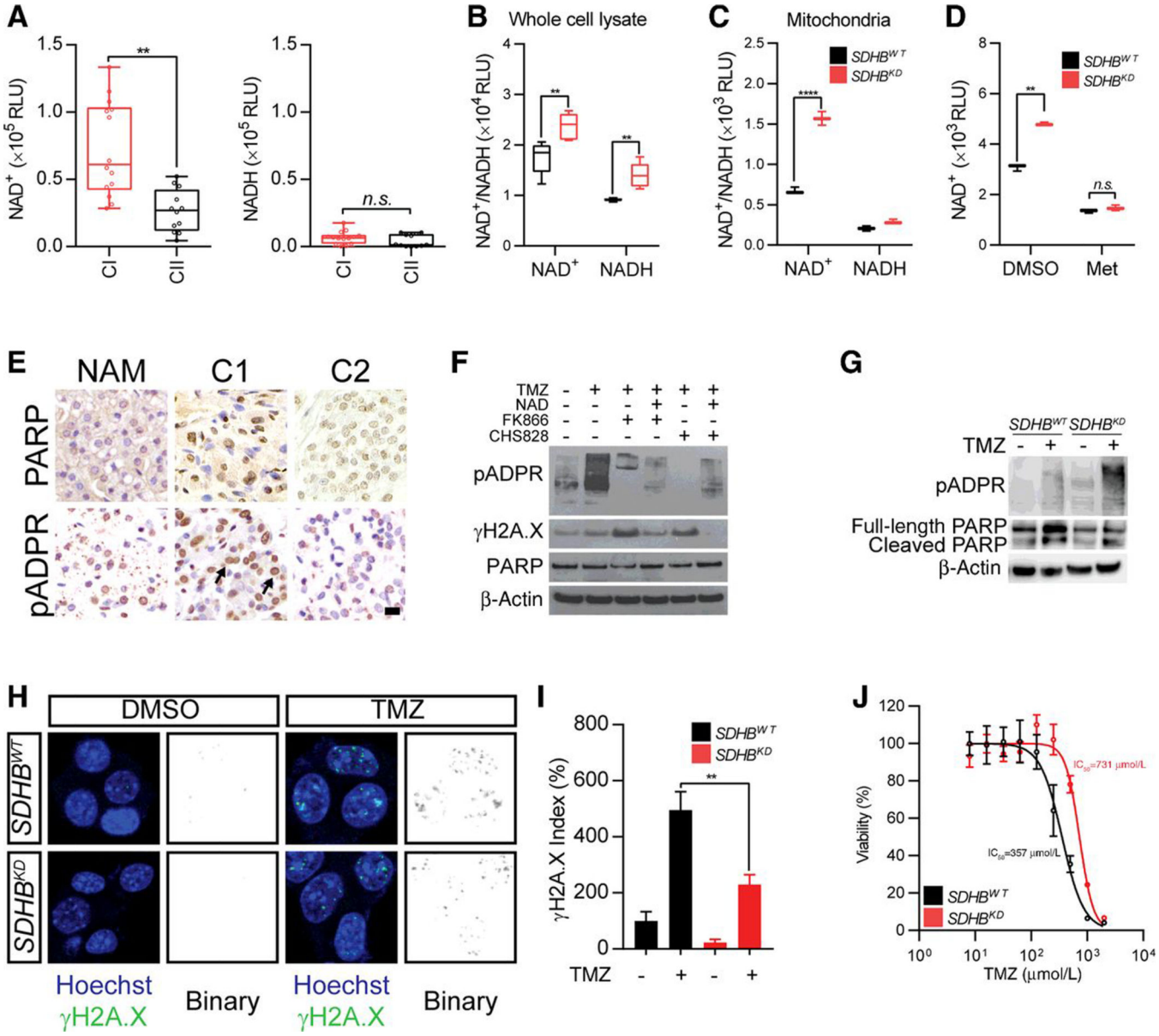

Figure 2.

Mitochondrial complex I addiction potentiate chemoresistance through PARP DNA repair pathway. **A,** NAD^+/NADH quantification in CI and CII PCPG. **, $P < 0.01$. **B,** NAD^+/NADH quantification in whole-cell lysate in MTT cells. **, $P < 0.01$. **C,** NAD^+/NADH quantification in isolated mitochondria from MTT cells. **, $P < 0.001$. **D,** NAD^+ quantification in MTT cells in the presence of mitochondrial complex I inhibitor metformin (Met). **, $P < 0.01$. **E,** Immunohistochemistry of PARP and pADPR in CI and CII PCPGs. Bar, 10 μm. **F,** Western blot for pADPR expression in MTT cells treated with Nampt inhibitor FK866 and CHS828. β-Actin was used as loading control. **G,** Western blot for pADPR, PARP, and cleaved PARP1 expression in MTT cells treated with temozolomide (TMZ) showed PARP activity is higher in *SDHB* knockdown cells and less cleaved PARP in *SDHB* knockdown cells. β-actin was used as loading control. **H,** Immunostaining for

γH2A.X puncta in MTT cells under TMZ treatment showed reduced DNA damage in *SDHB* knockdown cells. The signal of γH2A.X was shown in binary for clearance. **I,** Quantification for γH2A.X index in TMZ-treated MTT cells. **, $P < 0.01$. **J,** Dose–response curve showed cytotoxic effect of TMZ in MTT cells.

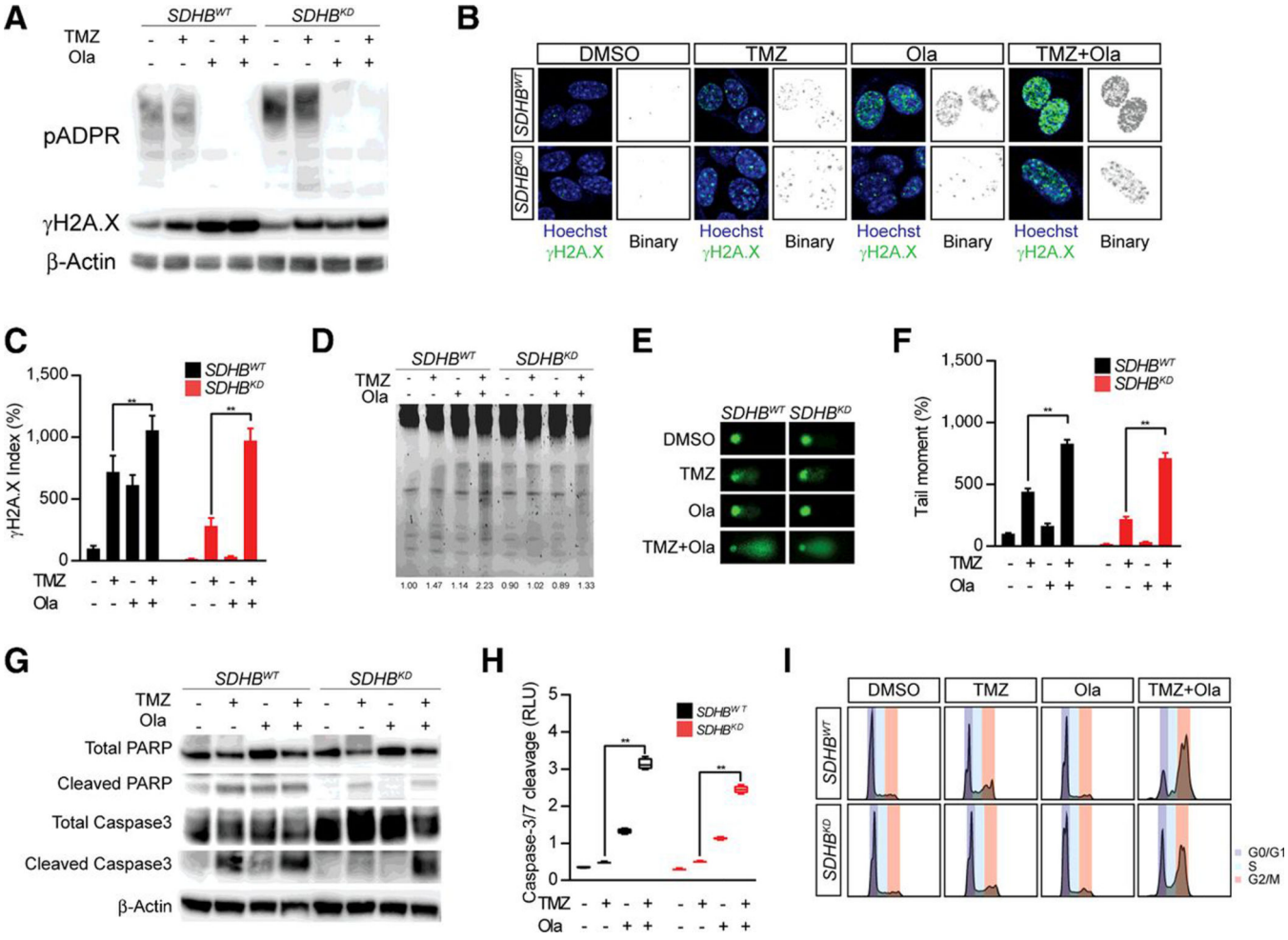

Figure 3.

Targeting PARP DNA repair pathway potentiate therapeutic effect of genotoxic agents. **A,** Western blot for pADPR and γH2A.X expression in MTT cells treated with TMZ and Olaparib (Ola). TMZ induces more pADPR formation in *SDHB* knock down cells and Ola increased γH2A.X expression under TMZ treatment. β-Actin was used as loading control. **B,** Immunostaining for γH2A.X in MTT cells treated with TMZ and Ola showed Ola enhanced γH2A.X signal under TMZ treatment. The signal of γH2A.X was shown in binary for clearance. **C,** Quantitative analysis for γH2A.X index. **, $P < 0.01$. **D,** DNA fragmentation test for MTT cells treated with TMZ and Ola. Combined Ola and TMZ treatment resulted in more fragmented DNA. **E,** Comet assay measuring DNA fragmentation in MTT cells treated with TMZ and Ola. **F,** Quantification of comet tail moment in MTT cells. **, $P < 0.01$. **G,** Western blotting for PARP1, cleaved PARP1, caspase-3, and cleaved caspase-3 in MTT cells treated with TMZ and Ola showed Ola plus TMZ combination therapy led to marked increase of cleavage of PARP and caspase-3. β-actin was used as loading control. **H,** Caspase-3/7 Glo assay for MTT cells treated with TMZ and Ola showed Ola-increased TMZ-induced apoptosis. **, $P < 0.01$. **I,** Cell-cycle analysis for MTT cells treated with TMZ and Ola. Increased G_2–M arrest under TMZ and Ola combined treatment.

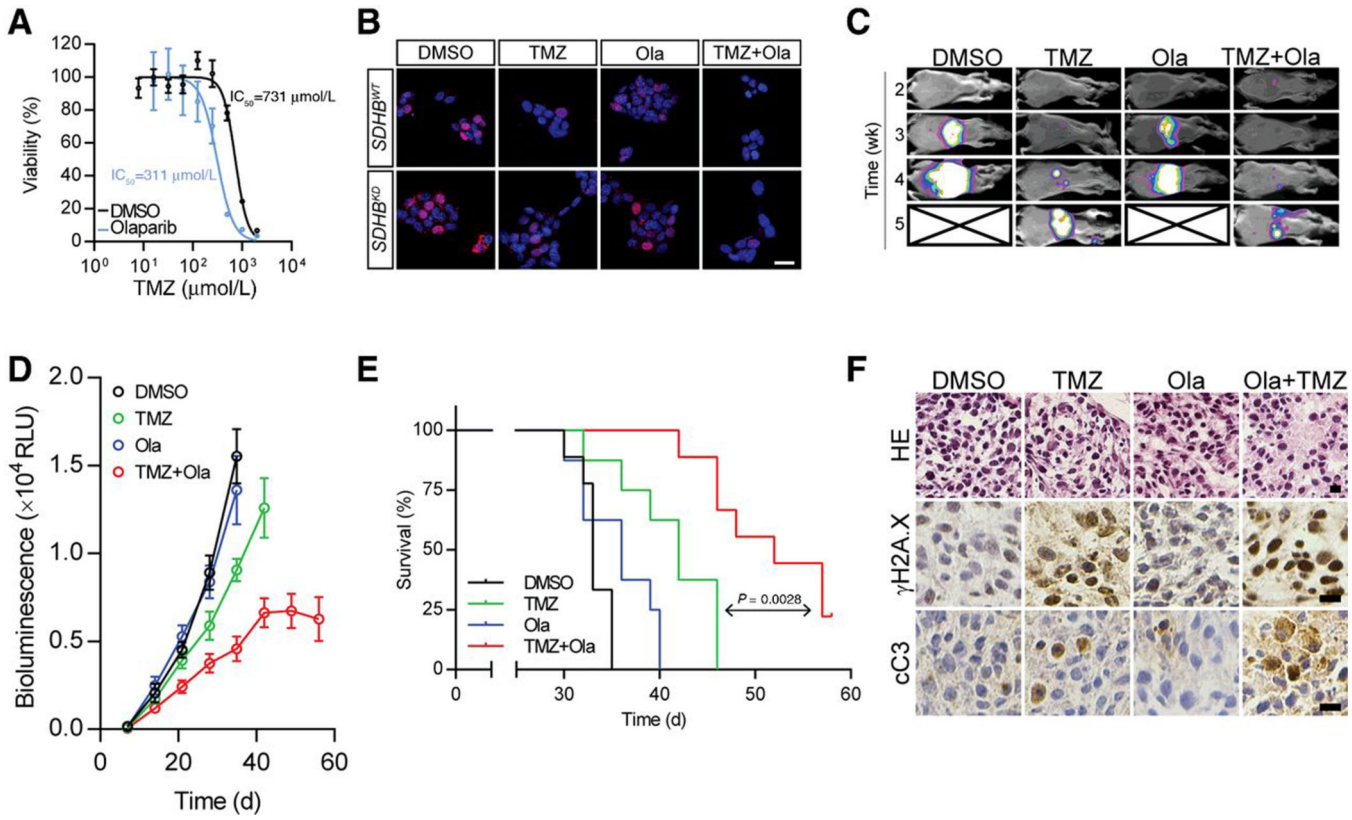

Figure 4.

Combination of PARP inhibitor and TMZ reduces metastatic lesion and prolongs overall survival. **A,** Cell viability test of *SDHB*^{KD} cells under combination of TMZ and Ola showed Ola reduced the IC50 of TMZ. **, $P < 0.01$. **B,** BrdUrd incorporation test for MTT cells treated with TMZ and Ola showed Ola resulted less BrdUrd incorporation. Bar, 10 μm. **C,** *In vivo* bioluminescence assays of mice bearing MTT-*SDHB*^{KD}-Luc cells under DMSO, Ola, TMZ or combination treatments. **D,** Quantification of the bioluminescence signals by the IVIS system. **E,** Survival curve of mice bearing MTT-*SDHB*^{KD}-Luc cells under DMSO, Ola, TMZ or combination treatments ($P = 0.0028$). **F,** Histology and expression of γH2A.X and cleaved caspase-3 (cC3) in tumor sections from mice bearing MTT-*SDHB*^{KD}-Luc cells under DMSO, Ola, TMZ or combination treatments. Bar, 10 μm.

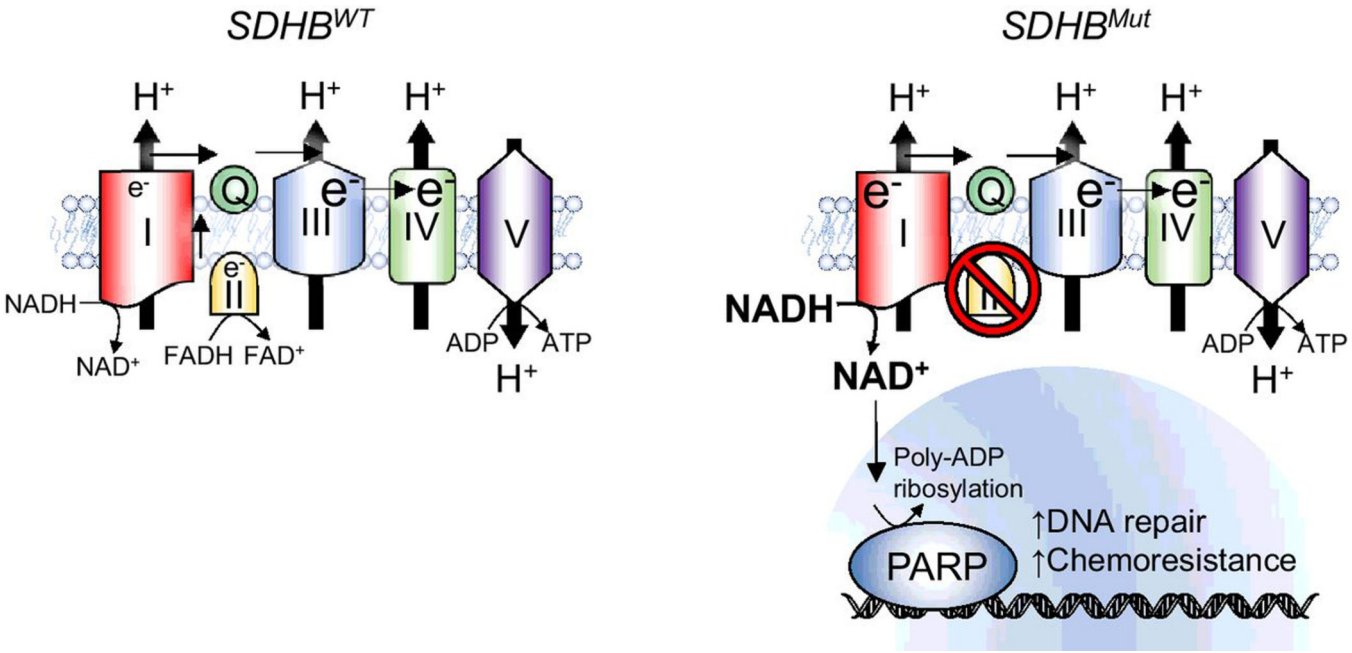

Figure 5.

Schematic illustration of SDHB deficiency-associated drug resistance. Left, mitochondrial complex I and II supply coenzyme Q with electron. Electron transport chain maintains mitochondrial membrane potential and ATP generation. Right, in cancer cells with *SDHB* genetic deficiency, the loss of mitochondrial complex II-derived electron results in dependency on complex I. Upregulated NADH dehydrogenase activity alters NAD^+/ NADH balance, resulting in increased NAD^+ availability and enhanced PARP DNA repair. Targeting NAD^+/PARP DNA repair pathway sensitizes SDHB-deficient PCPG to genotoxic agent such as TMZ.